Measurement and Modeling of Multi-user Multi-antenna system in Aircraft in the Presence of Electromagnetic Noise and Interference

Sai Ananthanarayanan P.R., *Student* Member*, IEEE,* Alyssa Magleby Richards, *Student* Member*, IEEE*, Cynthia Furse, *Fellow, IEEE*

Abstract

This paper evaluates the accuracy with which the performance of a multi-user multi-antenna system can be predicted with and without considering co-channel interference and noise (Gaussian, α-stable and Cauchy) using a site-specific 3D ray-tracing algorithm as well as with statistical models with Gaussian and Nakagami-m channel models in small to medium sized aircraft. These models expand on previous statistical channel models such as the hyper-Rayleigh model by including the simultaneous effects of co- and adjacent channel interference, antenna matching, efficiency, directivity and polarization as well as (for the 3D model) site-specific multipath effects. Measurements and comparisons are made in a metallic-bodied Beech Baron BE 58P and a composite structure Rockwell T-39 Sabreliner. It was found that the 3D ray tracing model provides a mean capacity within 1 % of those measured in the two aircraft in the presence of interference and noise. This was closely followed by the Nakagami-m distribution (m=1.4) which was within 1-3% of measured capacity in the presence of interference and within 6% for a combination of interference and noise and the Gaussian model which was within 6% of measured capacity in the presence of interference and within 11% for a combination of interference and noise . The Cauchy noise degraded the capacity more than the other types of noise in the aircraft, providing a lower bound for capacity in an aircraft system.

I. Introduction

Multi-antenna (MU) communication systems are being developed to satisfy the future demands of high-speed data transfer across wireless networks. Traditional single user multi-antenna systems pose many practical limits on the potential throughput of data in a downlink with many active users. The emergent

UU IR Author Manuscript

field of multi-user multi-antenna system is therefore gaining a great deal of interest for its ability to efficiently transfer data to many independent users at once. Due to its intrinsically rich multipath and potential for many simultaneously active users, the aircraft cabin is a potentially well suited application for multi-user multi-antenna technology. With the emergence of broadband wireless data access on airlines, there is naturally an increasing demand for greater transfer rates of dataPrevious results in [1] have provided an overview of measured multi-user multi-antenna systems for aircraft and have provided a comparison between the measured and simulated MU capacity for a Rockwell T-39 Sabreliner small aircraft. The results in [1] showed a good agreement between measurements and a 3D ray tracing model. Although the 3D model is a great tool for analyzing the aircraft system it requires detailed information about the locatoin of walls, chairs, people, etc. in the aircraft fuselage.. This paper explores the possibility of using simpler statistical models for analyzing wireless communication in this aircraft. Statistical models such as the hyper-Rayleigh [2] and IEEE 802.11 TGn [3] channel models have been used for analyzing both single and multi-antenna system in aircraft. In addition Weibull and Nakagami-m models have been used for studying single antenna systems in aircraft [4][5]. This paper examines the accuracy of the Gaussian and Nakagami-m statistical models and the site-specific 3D ray-tracing model for analyzing MU-multi-antenna systems in two small aircraft: Beech Baron BE 58-P and the Rockwell T-39 Sabreliner.

For accurate capacity prediction both co-channel and adjacent channel interference along with environmental and system noise must be considered. This is particularly true in applications where users are tightly packed (such as in airplanes, buses, buildings, and crowds), where external noise is significant (in aircraft, near other broadcast centers, in industrial plants, etc), where communication is particularly sensitive or critical (hospitals, military applications). Interference models have been developed in the past for analyzing single-user multi-antenna systems in a tunnel [9] and other indoor and outdoor wireless applications [8]. MU-antenna system interference has been studied for wireless communication in indoor and outdoor environments. Statistical interference modeling for MU-MIMO systems has been performed using game theory analysis in [13], and a general extension of single user MIMO interference to MU

UU IR Author Manuscript

system is found in [14][13]. In this paper we will extend the network theory based interference and noise model developed for tunnels to analyze MU multi-antenna systems in aircraft.

Noise in a wireless system includes both environmental noise and system level noise. Gaussian noise is the most commonly used model for noise in both single and multi-antenna system, and will be evaluated in this paper. [refs] However, in aircraft impulsive noise may be far more common. Middleton [15] and Blum [16] were the first to formulate the impulsive non-Gaussian noise in many indoor and outdoor communication environments for single and multi-antenna systems, respectively. Bhatti [17] studies the effect of impulsive noise on a WLAN environment and shows that narrowband impulsive noise is more benign than additive white Gaussian noise in both moderately and highly impulsive environments. This paper studies the effects of both Gaussian an α-stable noise with various levels of impulsiveness on the capacity measurements performed on the two aircraft. Four different values of the characteristic exponent α (1.5, 1.2, 1.1, and 1) are analyzed. Section III briefly describes the system model for multi-user multi-antenna systems in the presence of interference and noise. Section IV provides a detailed explanation of the multi-antenna measurement setup in aircraft for measuring system capacity with and without interference and noise. Section V compares the capacity obtained using the measurements in the aircraft system to those predicted using the 3D ray-tracing model and the statistical models with and without interference in aircraft.

II. AIRCRAFT CHANNEL MODELING

Channel modeling is important to predict the capacity of wireless communication systems in different environments. Various channel models based on both statistical modeling as well as 3D ray-tracing have been proposed for analyzing wireless systems in aircraft. [3][6][7] The Nakagami-m model and the Gaussian channel models and a site specific 3D ray-tracing model have been found to be the most accurate of these models for our application, [ref] .

Among the simplest models is the Gaussian channel model, which specifies a plane of impinging waves with Gaussian-distributed magnitudes and uniformly distributed AOAs and phases. The Gaussian

UU IR Author Manuscript

channel provides a approximation to the aircraft channel, but the Nakagami model provides even better estimates for multi-antenna systems in aircraft. [4] The Rayleigh and uniform distribution on the unit circle are special cases of Nakagami model with m=1 and m=∞ respectively. The received signal can be written as

$$\beta_k = R_k \exp(j\Theta_k) \tag{3}$$

R_k has a pdf distribution given by

$$p_R(r) = \frac{2m^m r^{2m-1}}{\Omega_m \Gamma(m)} \exp(-\frac{mr^2}{\Omega}) \tag{4}$$

where m is the shape parameter and Γ is the spread parameter. The results in this paper were obtained for an m of 1.4 which was found empirically to be the most accurate for the aircraft under consideration.

In addition to accurately predicting the communication channel which includes channel parameters like the path loss, angle of arrival (AOA), angle of departure (AOD), and system level parameters such as the antenna directivity ($\boldsymbol{D}_R$), polarization ($\boldsymbol{P}$), efficiency at both transmitter ($\boldsymbol{E}_{\text{cdt}}$) and receiver ($\boldsymbol{E}_{\text{cdr}}$), matching at transmitter ($\boldsymbol{M}_T$), and receiver($\boldsymbol{M}_R$), and spatial correlation of the signals impinging on the receiver is given as $\boldsymbol{R}_s$ are also included. These parameters are used for developing a detailed signal model where the complete channel model **H** can be given as:

$$\mathbf{H} = \underbrace{\underbrace{Z_0^{1/2} \underbrace{\mathbf{S}_{21}(\mathbf{I}-\mathbf{S}_{RR}\mathbf{S}_{11})^{-1}}_{matching}\left(\mathbf{I}+\frac{\mathbf{Z}_{RR}}{Z_0}\right)^{-1}}_{M_R} \underbrace{\mathbf{E}_{cdr}}_{\substack{rad\\eff}} \underbrace{\mathbf{S}_{RT}}_{H_{DP}} \underbrace{\mathbf{E}_{cdt}}_{\substack{rad\\eff}} \underbrace{(\mathbf{I}-\mathbf{S}_{TT})}_{matching}}_{M_T}, \tag{1}$$

$$\mathbf{S_{RT}} = \sum_{i=1}^{N_R}\sum_{j=1}^{N_T}\left[\frac{1}{Z_0}\sum_{k=1}^{N_p} E_i^R(\theta,\phi)\beta_k E_j^T(\theta,\phi)\right] \tag{2}$$

where Z_0 is the characteristic impedance, $\boldsymbol{S}_{TT}$ and $\boldsymbol{S}_{RR}$ are the scattering parameters of the unloaded transmit and receive arrays respectively, $\boldsymbol{S}_{RT}$ is the channel scattering matrix, and $\boldsymbol{S}_{11}$ and $\boldsymbol{S}_{21}$ represent a matching circuit and transmission circuit for a selected matching approach. The influence of the channel on channel-system capacity is expressed as a summation of N_p plane waves where the k^{th} plane wave has

complex gain (path loss and phase shifts) β_k. The ***S*** and the ***Z*** parameters in (1) were obtained by simulating the antennas along with the ground plane using an electromagnetic solver using full wave finite integration technique (FIT) called CST. The path loss in this paper will be modeled using a Gaussian, Nakagami-m or 3D ray tracing channel.

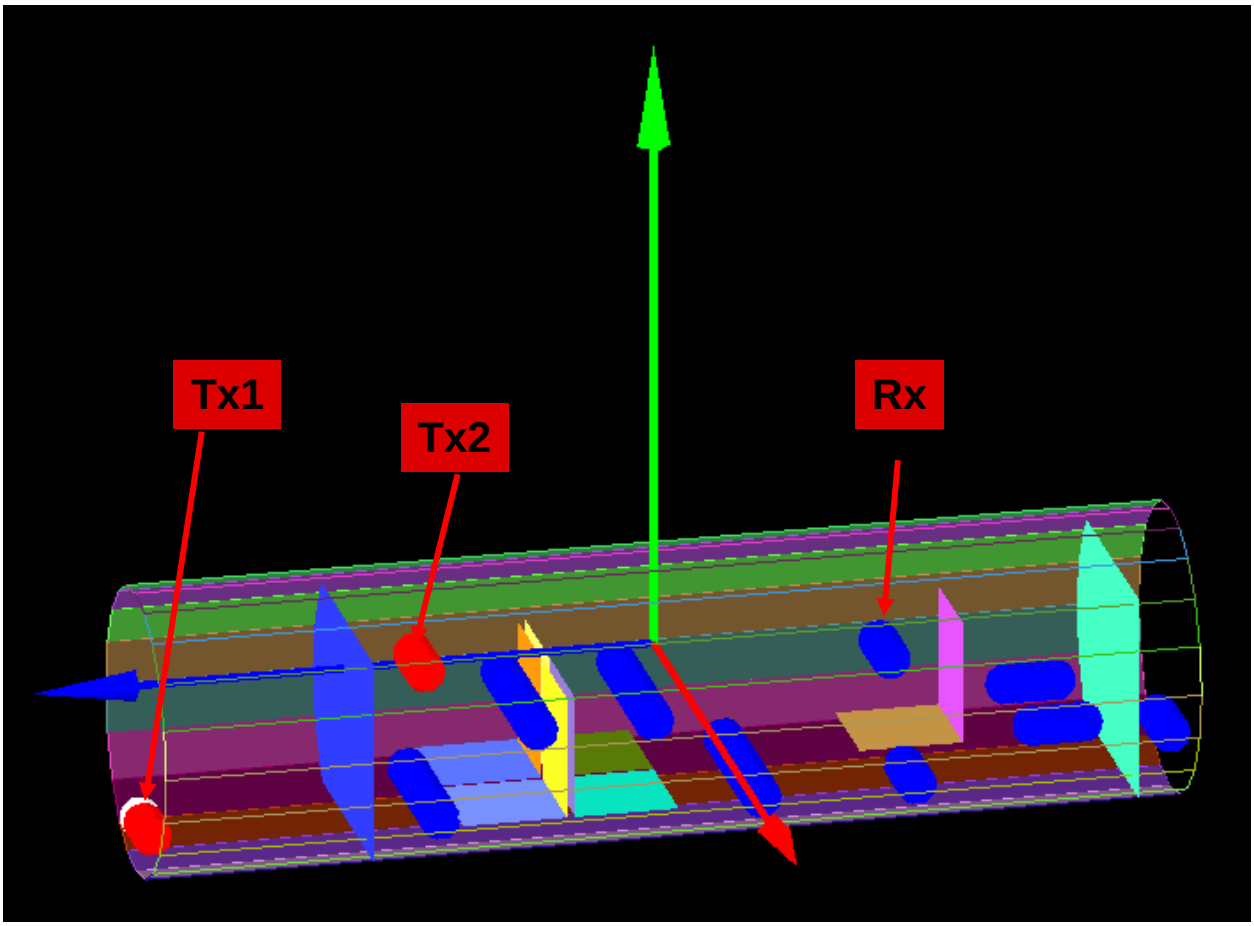

Figure 1: Simple 3D rendering of the interior of the Beech Baron 58P aircraft using the 3D ray-tracing software. The aircraft is modeled as a faceted 3D cylinder with capped ends. The little spheres represent transmit and receive antennas

A 3D ray-tracer was used to provide site-specific channel models. This method uses a triangular grid to determine which rays arrive at the receive antenna [7]. The algorithm uses 30% or less CPU time than traditional ray-tracing methods and has been validated in 2D environments for indoor and outdoor multipath environments and in a 3D environment for reflections in stairwells[18][19]. The software was adapted to a multi-antenna system by running the ray tracer multiple times for different antenna locations rather than just a single set at a time. The two aircraft were modeled with 20 faceted sides to represent the

cylindrical shape of the fuselages and flat rectangular surfaces for the front and back of the fuselages. Figure 1 shows a screen shot of the ray-tracer inside the Beech Baron BE 58P. The floor was assumed to be electrically invisible. Lossy and reflective internal obstacles such as chairs, reflective walls, etc. were fully configurable. Material properties were also configurable, allowing specific permittivity and conductivity to be entered for reflective objects and the loss factor in dB to be entered for lossy objects. All aircraft walls were assumed to be perfect electrical conductors (PEC). Chairs were modeled as two flat surfaces connected at one edge with a loss factor of 0.1 dB. This loss factor was estimated based on chair measurements made in an anechoic chamber at 915 MHz. Lossy walls within the cabin were modeled as a rectangular surface with a loss factor of 2.6 dB, which was found to give the most accurate results when varying the wall loss and omparing to measured values. The transmitter and receiver locations were configurable. The maximum number of projected rays was 320 which were attained when 15 or more bounces occur before a ray reaches the receiver.

The complex electric fields and angle of arrival and departure for each antenna pair were computed. These were post processed to rearrange the data into the channel matrix, which was then used to calculate capacity using (1) by replacing $\boldsymbol{S}_{RT}$ with the channel matrix obtained using the ray-tracing model. The received power at each angle of arrival was used along with the antenna parameters to obtain the 3D channel matrix $\boldsymbol{H}_{3D}$ which is then used for obtaining the channel matrix '$\boldsymbol{H}$' given as:

$$H = \underbrace{\underbrace{Z_0^{1/2}\underbrace{S_{21}(I - S_{RR}S_{11})^{-1}}_{matching}\left(I + \frac{Z_{RR}}{Z_0}\right)^{-1}}_{M_R}\underbrace{E_{cdr}}_{\substack{rad\\eff}}\underbrace{[H_{3D}]}_{H_{DP}}\underbrace{E_{cdt}}_{\substack{rad\\eff}}\underbrace{(I - S_{TT})}_{matching}}_{M_T}}_{H}, \tag{5}$$

where H_{3D} includes the channel path loss along with the gain at both the transmitter and receiver. The channel models described in this section will be used for analyzing MU multi-antenna system in Section V.

III. MEASUREMENTS

Measurements were performed on two aircraft using the University of Utah multi-antenna test bed [20]. Measurements were first taken in a Beech Baron BE 58P which is a typical metallic-bodied small commuter aircraft (29.8 feet from nose to tail). Two transmitter locations were chosen on the aircraft and are depicted in Figure 2. Transmitter Tx1 was placed in the front luggage compartment in the nose of the aircraft, and transmitter Tx2 was placed on the copilot dashboard. The receiver locations were chosen to cover the interior of the cabin as uniformly as possible, thus providing a comprehensive survey of the interior. A mapping of these locations is shown in Figure 2.

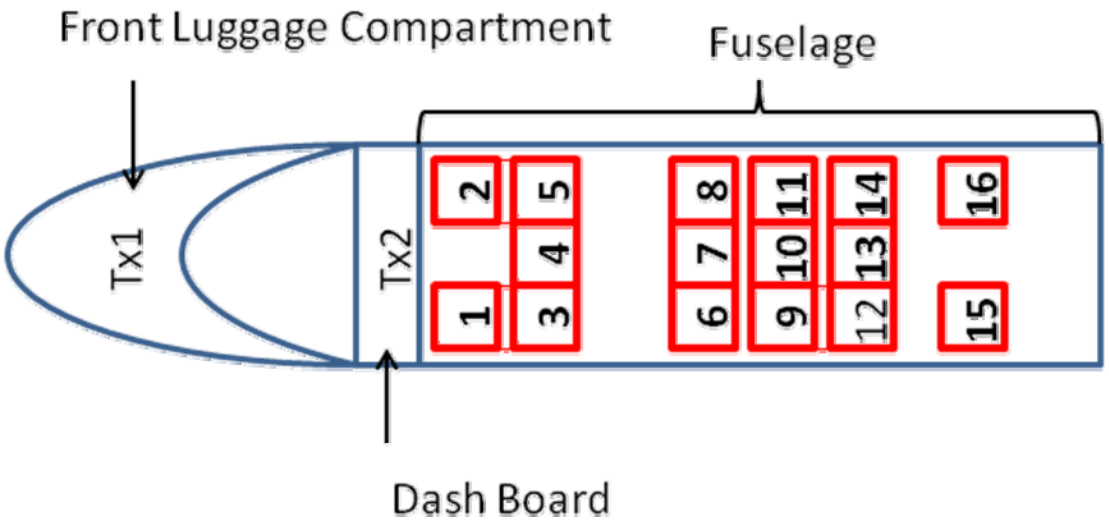

Figure 2 : The Beech Baron BE 58P. Test locations for the transmit array are marked with numbered boxes. Tx1 was placed in the luggage compartment in the front nose. Tx2 was placed in the front dashboard. Rx1-Rx16 are located inside the fuselage.

Measurements were then taken in a Rockwell T-39 Sabreliner which is a typical mid-size commuter aircraft (47 feet from nose to tail) with a composite body. Three transmitter locations were chosen throughout the aircraft, and are depicted in Figure 3. The first location (Tx1) was placed at the center of the dashboard in the cockpit. The second location (Tx2) was placed within a maintenance bay underneath the tail. The third location (Tx3) was placed in a centralized location within the cabin. The receiver locations were chosen to cover the interior of the cabin as uniformly as possible as shown in Figure 3.

UU IR Author Manuscript

After placing the receive array at its specified location, a training packet of data was broadcast by the transmit array, thereby providing a direct measurement of the channel matrix for that given transmitter/receiver pair. The receive array was then moved to the next location, and another packet was transmitted. This cycle was repeated until the survey of the interior was complete. As long as the environment within the cabin was unchanged over the measurement cycle, all channel matrices may be treated as if they were obtained simultaneously.

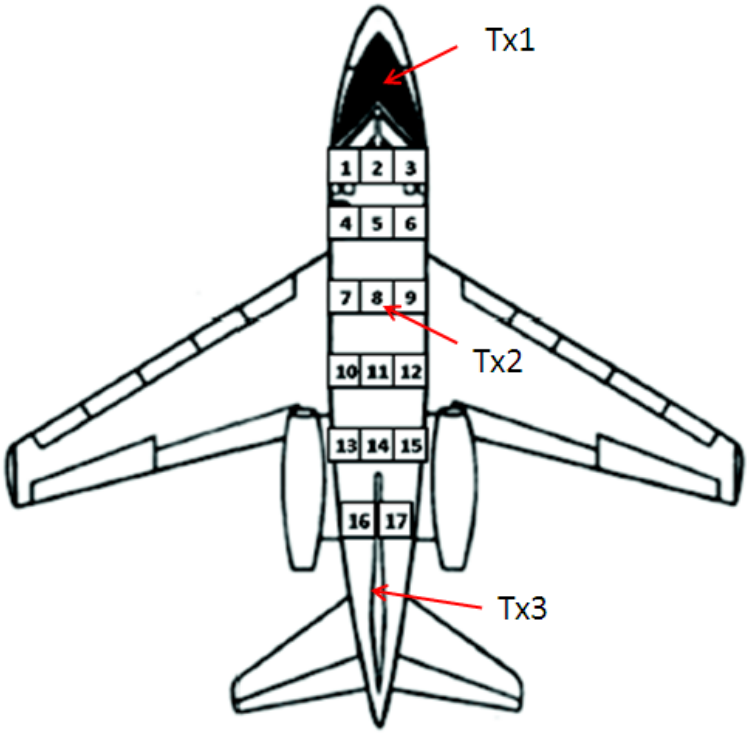

Figure 3: The Rockwell T-39 Sabreliner. Test locations for the transmit array are marked with numbered boxes. Tx1 was placed in the dashboard of the cockpit. Tx2 was a maintenance bay in the tail. Rx1-Rx17 are located inside the fuselage. Tx3 is located at location Rx8 in the center of the fuselage.

These measurements provided a direct measurement of the channel matrix for each transmitter/receiver pair. For the Beech Baron BE 58P, Tx2 was used as interferer. For the Rockwell T-39 Sabreliner, Tx2 and Tx3 acted as interferers (operating sequentially). The signal was sampled using the test bed as before, and the channel matrix for the interferers was obtained.

A fortunate aspect of channel capacity measurement is that one need not physically implement a given algorithm in order to calculate its potential capacity. In fact, the only requisite measurement is a set

of H-matrices for the various test locations. It is therefore important to understand how a channel matrix is computed from a packet of data. We begin by defining a complex *M* x *W* matrix *T*, called the training sequence, and write it as a series of column vectors with the form

$$T = [\, t(1)|\ t(2)|\ \_\ \_\ \_\ |t(W)\,] \qquad (6)$$

In other words, each column vector t(*w*) represents an M x 1 vector of complex data symbols being broadcast by the transmitter at time . The N x W matrix of sampled symbols at the k^{th} receiver may therefore be written as

$$Y_k = H_k T + N_k \qquad (7)$$

where, N_k is simply an *N* x *W* matrix of sampled noise. Because *T* is a known sequence of data, it can be used to estimate the channel matrix. Defining the matrix

as the channel matrix estimate, we may simply write:

$$\widetilde{H}_k = Y_k T^+ = H_k + N_k T^+ \qquad (8)$$

where T^+ denotes the Moore-Penrose pseudo inverse of *T*, and is given by

$$T^+ = (T^H T)^{-1} T^H \qquad (9)$$

As long as the SNR at the receiver is relatively large, the effects of the noise term N_k are negligible, and $\widetilde{H}_k$ transforms to H_k. The effects of noise may be further reduced by choosing a relatively large value for W. This is because the quantity $N_k T^+$ behaves much like a correlation between the training sequence and the noise. Thus, in the limit as W$\rightarrow\infty$, we have $N_k T^+ \rightarrow 0$ for uncorrelated noise. So as long as the channel itself remains stationary over the duration of the training sequence, *W* may be chosen as any arbitrarily large value. For the data presented in this paper, all channel matrices were estimated using a training sequence of pseudorandom data with length W = 4000.

IV. Interference and Noise in Multi-Antenna System

This section derives the complete model for single user interference and noise in a multi-antenna system for additive white Gaussian, α-stable noise and impulsive noise having a Cauchy distribution. This model can be easily extended to MU multi-antenna system and will be discussed in the following section. If we assume L co-channel interferers in an aircraft system, the total received signal for a system in the presence of interference and both Gaussian and non-Gaussian noise can be formulated as:

$$y = Z_o^{1/2} S_{21} (I - S_{RR} S_{11})^{-1} (I + \frac{Z_{RR}}{Z_o})^{-1} E_{cdr} [[\frac{1}{Z_o} \sum_{k=1}^{W_i} E_i^R (AOA_{k,L}, r) p_r \beta_{k,L} e_j^T (AOD)_{k,l}] E_{cdt,L} (I - S_{TT,L}) x_L + \sum_{a=1}^{L-1} [\frac{1}{Z_o} \sum_{k=1}^{W_i} E_i^R (AOA_{k,a}) p_r \beta_{k,a} e_j^T (AOD)_{k,l}] E_{cdt.a} (I - S_{TT,a}) x_a + N^{\alpha} + N^g \quad (11)$$

where there are W_i signals impinging on each receiver, N^{α} is the α-stable noise, and N^g is the Gaussian noise. The AWGN noise is given by

$$N^g = \sigma^2 I \quad (12)$$

where σ is the noise variance. The symmetric α-stable distribution is defined by the characteristic function

$$\varphi(\omega) = \exp(j\delta\omega - \gamma |\omega|^{\alpha}) \quad (13)$$

where α is the characteristic exponent that controls the heaviness of the tails of the stable density, δ is the location parameter, $\varphi(\omega)$ is a function of ω, and γ is the dispersion parameter. For a standard distribution δ=0. For a bivariate symmetric α-stable noise distribution we have

$$\varphi(\omega_1, \omega_2) = \exp(-\gamma |\omega_1^2 + \omega_2^2|^{\frac{\alpha}{2}}) \quad (14)$$

When α=2 the distribution becomes Gaussian, and when α=1 the distribution becomes Cauchy. The α-stable noise is added to the measured data stream for various values of α and γ=0.1 using a complex isotropic symmetric α-stable (*SαS)* random variable as in [21].

V. Capacity in Multi-User Multi-Antenna System with Interference and Noise

This section discusses three methods for analyzing MU-multi-antenna systems. The first method based on dirty paper coding (DPC) provides the maximum achievable capacity for a MU system in the presence of noise. The second method based on linear precoding and the third method based on time division multiple access (TDMA) can be implemented in real time. There are many other detectors, all of which involve some sort of tradeoff between these two metrics and therefore tend to fall in between the DPC and TDMA extremes.

a) Time Division Multiple Access

The time domain multiple access (TDMA) based system is the simplest to implement. In this method each user is allotted a unique time window for transmitting information and the entire frequency spectrum is allotted to that user. The capacity for user *k* using TDMA in the presence of external interference is given by the well known water filling capacity which is

$$C_k = \max \log_2 | \mathbf{I} + \rho \mathbf{H}_k \mathbf{Q}_k \mathbf{R}^{-1} \mathbf{H}_k^H | \tag{15}$$

where **R** is given as

$$R = I + \sum_{j=1}^{L-1} M_R E_{cdr} H_{DP} E_{cdt,j} Q_j (M_R E_{cdr} H_{DP} E_{cdt,j})^H \tag{16}$$

The matrix **I** is the N X N identity matrix, and ρ is the average transmit symbol power to received noise ratio. The matrix Q_k denotes the transmit correlation matrix for user *k*, which is subject to trace $(Q_k) \leq \rho$, Although TDMA is relatively simple to implement, it does not provide the maximum achievable capacity for a MU-MIMO network. The reason for this is the idleness of the other *k*-1 users, who can drastically increase the throughput of the system by receiving their own independent, parallel bit streams. The true capacity for a multiuser network is therefore found by maximizing the sum-rate capacity over all users at once, and one algorithm which achieves this capacity is called dirty paper coding (DPC) [11][12].

b) Dirty paper coding

To compute the system capacity with DPC we invoke a duality between downlink broadcast channels and the uplink channels. The sum-rate capacity under this assumption can be written as

$$C_{DPC} = \max \log_2 | I + \rho \sum_{k=1}^{K} H_k Q_k H_k^H | \quad (16)$$

where Q_k is the transmit correlation for user k. Computation of this capacity is rather involved, but may be readily achieved by utilizing the algorithms found in [11]. Physical implementation of DPC is also computationally intensive and cannot yet be achieved in real-time. Nevertheless, it is still a useful benchmark for characterization because it represents the absolute highest capacity that nature will allow. In the presence of external interference (15) can be rewritten as

$$C_{DPC} = \max \log_2 | \mathbf{I} + \rho \sum_{k=1}^{K} \mathbf{H}_k \mathbf{Q}_k \mathbf{R}^{-1} \mathbf{H}_k^H | \quad (17)$$

where **R** is the interference + noise term.

VI. RESULTS

This section first presents the MU capacity for the Beech Baron BE-58P and the Rockwell T-39 Sabreliner without including the effects of interference and noise. The measured MU capacities in the presence of interference are then compared to those obtained using the 3D ray tracing and the statistical models for the two aircraft. The effect of noise on capacity are studied using the measurements and the results obtained are compared with capacity obtained using the 3D ray tracing model.

a) DPC and TDMA capacity with no interference or noise

Figures 4 and 5 show the cumulative distribution function(cdf) of the measured capacity in the two aircraft. The capacity obtained using the DPC scheme is much higher than that obtained using the TDMA scheme, thereby illustrating the tremendous advantages of MU-MIMO that have yet to be exploited in aircraft. From figures 3 and 4 we observe that the capacity exhibits very little variability over the

permutations of users, as indicated by the relatively tight bounds on the CDF curves. This is indicative of a strong uniformity in multipath richness throughout the cabin. Finally, we also see that Tx3 for the Sabreliner and Tx2 for the Beech Baron provide higher capacity, indicating that a centralized position for the transmitter is optimum when broadcasting to multiple users at once.

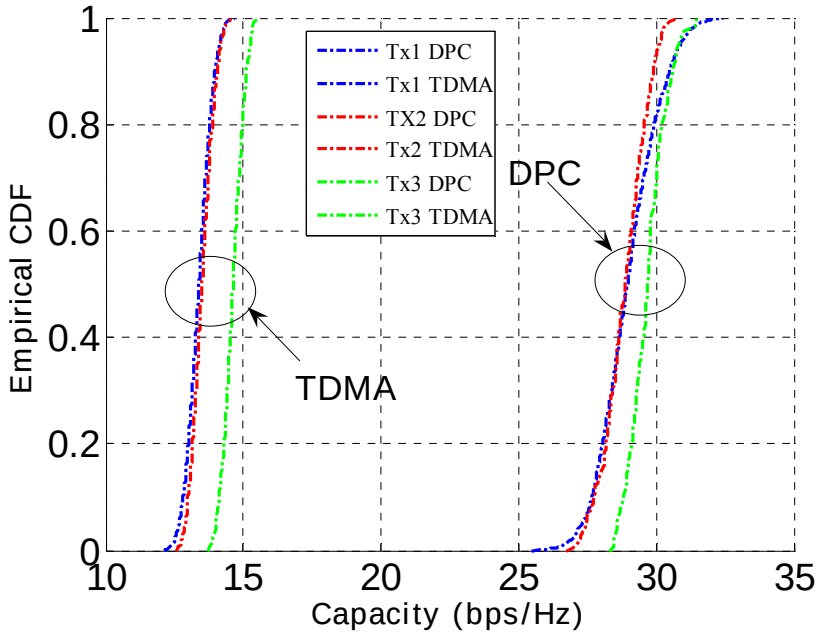

Figure 4: Empirical CDFs of the MU-MIMO capacities for the three transmitter locations in the Rockwell T-39 Sabreliner. The average SNR is fixed to Ps/Pn =20 dB.(The transmitter locations are shown in Figure 3)

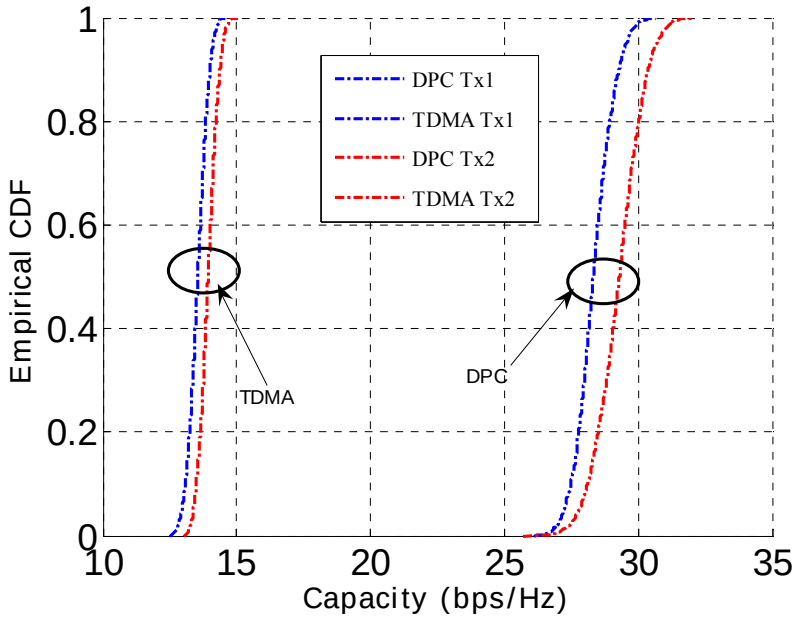

Figure 5: Empirical CDFs of the MU-MIMO capacities for the two transmitter locations in the Beech Baron BE 58-P. The average SNR is fixed to Ps/Pn =20 dB.(The transmitter locations are shown in Figure 2)

b) DPC and TDMA capacity in the presence of interference

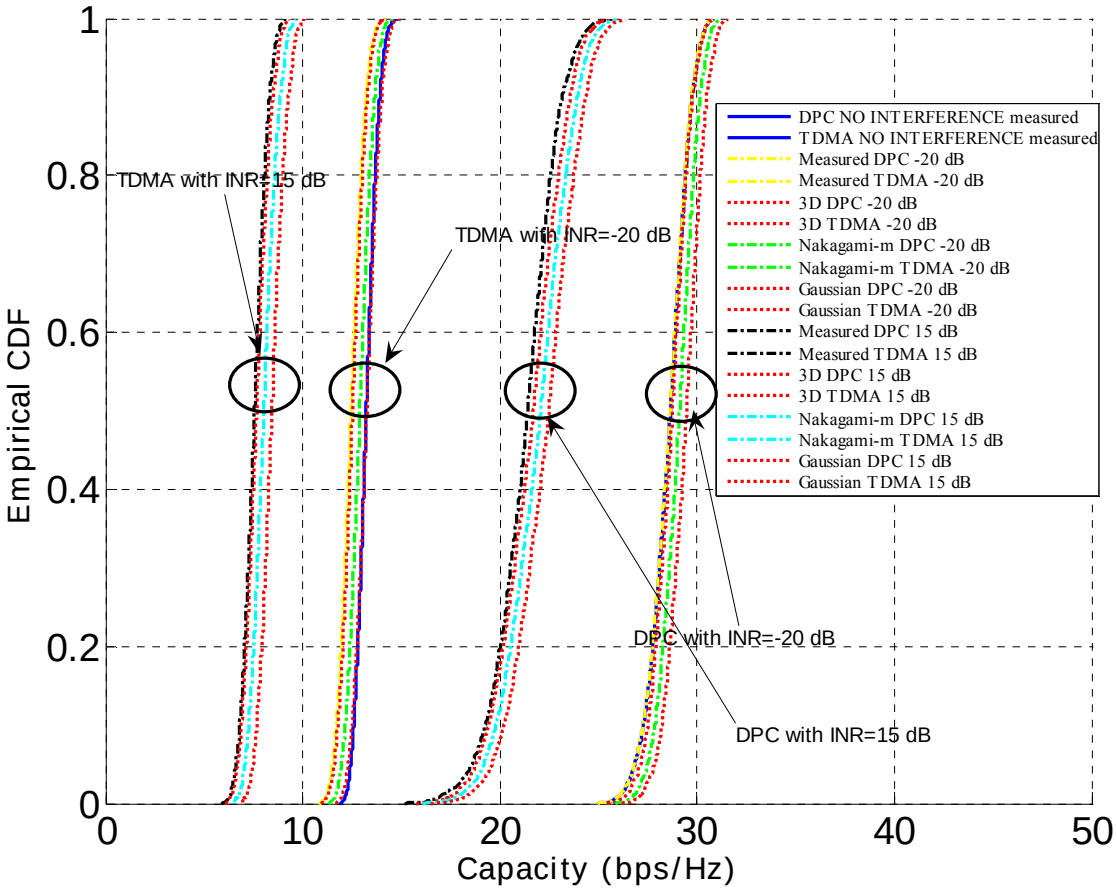

Figure 6: Empirical CDFs of the MU-MIMO capacities for the Rockwell T-39 Sabreliner with transmitter Tx2 acting as interferer. These capacities were obtained using measurements, 3D ray-tracing based Site specific modeling, and using statistical channel models like Nakagami-m and the Gaussian

Figures 6 and 7 show the cdfs of the measured capacity,3D ray tracing, and statistical model based simulated capacity for the Rockwell T-39 Sabreliner. Figure 8 shows the cdf for the measured and modeled capacity for the Beech Baron. The results in figures 6 and 7 were obtained by assuming the transmitters Tx2 and Tx3 acting as external interferes while figure 8 was obtained by assuming Tx2 as the external interferer. Two extreme values of interference to noise ratio (INR) viz: 15dB and -20dB were used for analyzing the MU system performance. Tables 1 and 2 summarize the mean capacity for the two interferers Tx2 and Tx3 for the Rockwell T-39 Sabreliner and the interferer Tx2 for the Beech Baron BE 58-P. From the tables we observe that the site specific 3D ray tracing software provides the best estimate

to the measured capacity in both aircraft. We also observe that the mean error between simulation and measurement for the 3D ray tracing method is less than 1 % for most cases for both the DPC as well as the TDMA method. We also see that the mean error for the Nakagami-m model is about 1-3% for both DPC and TDMA except for the TDMA method with INR of 15 dB where the error is about 6 %. The mean error for the Gaussian channel model is about 3-6% for both DPC and TDMA except for the TDMA method with INR of 15 dB where the error is about 10 %.

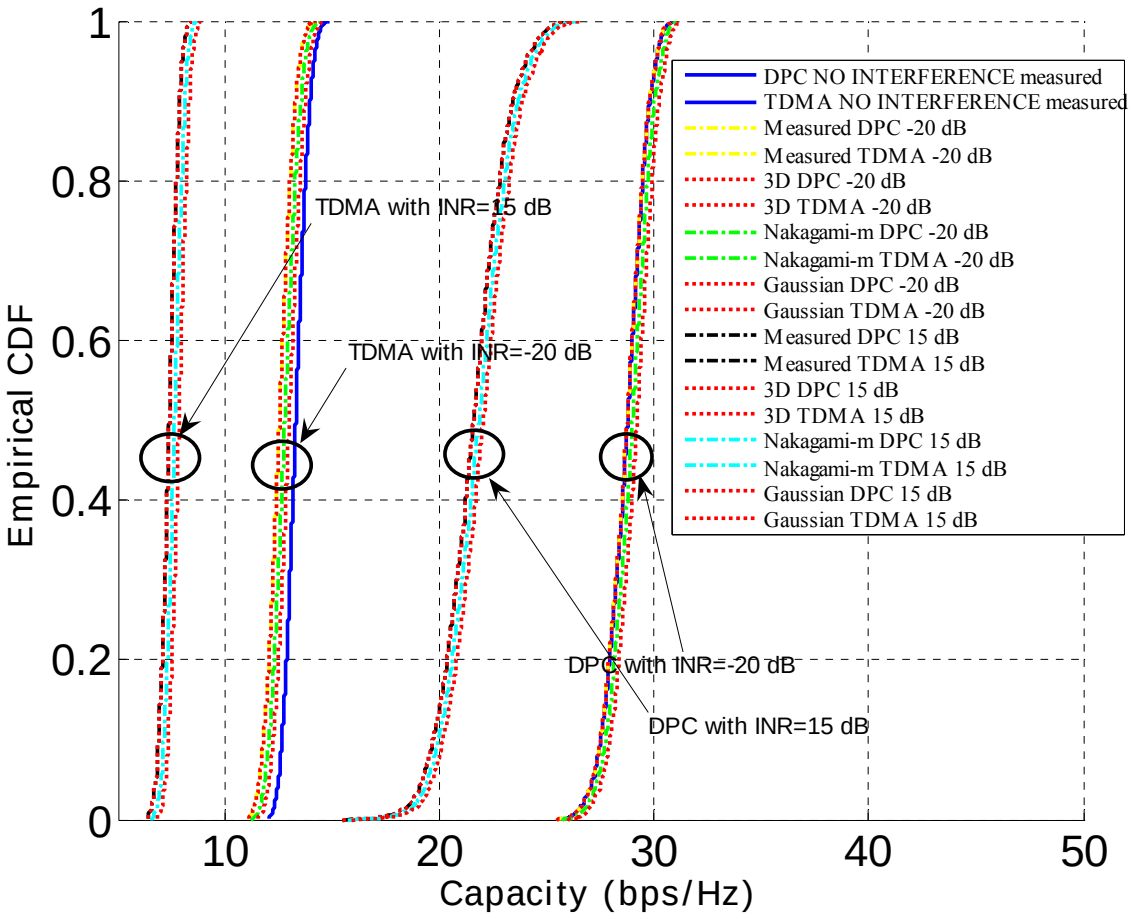

Figure 6: Empirical CDFs of the MU-MIMO capacities for the Rockwell T-39 Sabreliner with transmitter Tx3 acting as interferer. These capacities were obtained using measurements, 3D ray-tracing based site specific modeling, and using statistical channel models like Nakagami-m and the Gaussian

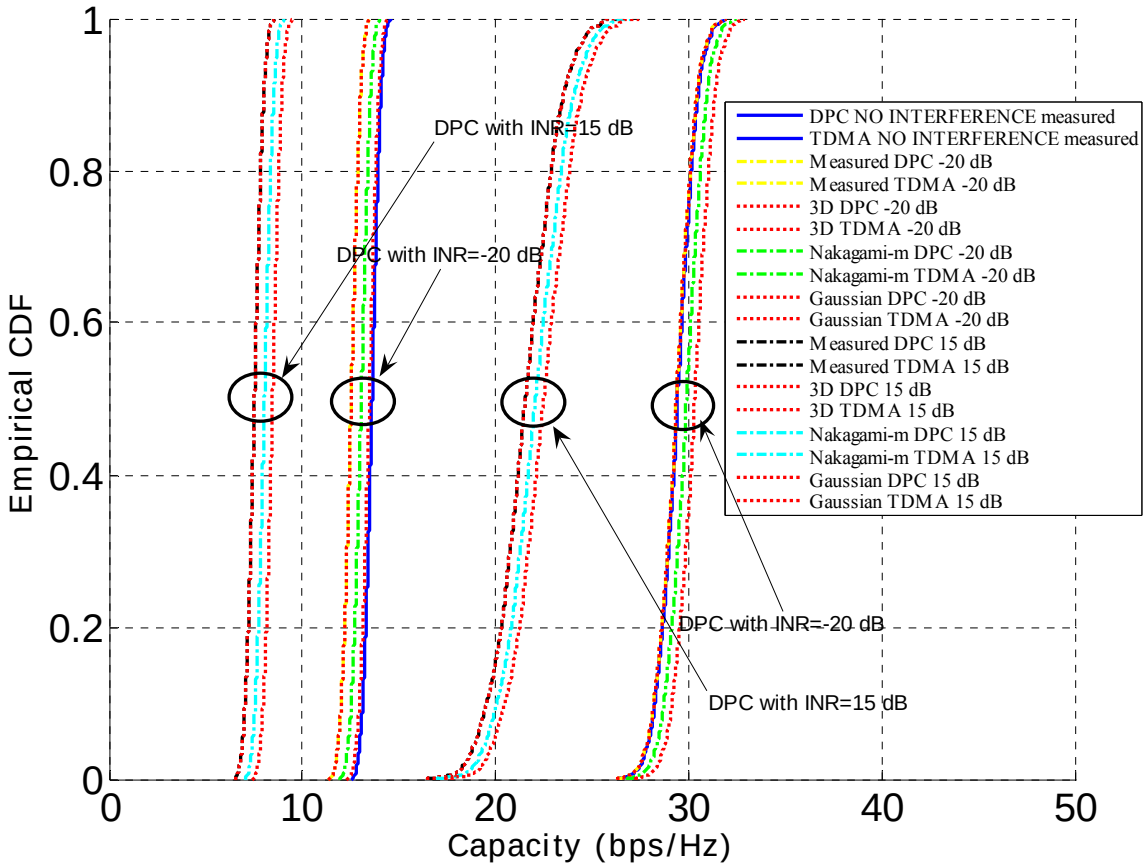

Figure 8: Empirical CDFs of the MU-MIMO capacities for the Rockwell Beech baron BE 58-P with transmitter Tx2 acting as interferer. These capacities were obtained using measurements, 3D ray-tracing based Site specific modeling, and using statistical channel models like Nakagami-m and the Gaussian

Table 1: Mean Capacity results for DPC and TDMA for INR of -20dB

INR= -20 dB	Measured Capacity DPC/TDMA (bits/sec/Hz)	3D ray tracing DPC/TDMA (bits/sec/Hz)	Nakagami-m DPC/TDMA (bits/sec/Hz)	Gaussian DPC/TDMA (bits/sec/Hz)
Sabreliner with Tx2 as interferer	28.5489/ 12.4556	28.6744/ 12.5333	29.0444/ 12.9033	29.3944/ 13.2533
Sabreliner with Tx3 as interferer	28.6775/ 12.5332	28.6790/ 12.5641	28.9235/ 12.7792	29.1295/ 12.9852
Beech baron with Tx2 as interferer	29.4078/ 12.5269	29.4659/ 12.6437	29.8744/ 13.0469	30.2944/ 13.4669

Table 2: Mean Capacity results for DPC and TDMA for INR of 15 dB

INR= 15 dB	Measured Capacity DPC/TDMA (bits/sec/Hz)	3D ray tracing DPC/TDMA (bits/sec/Hz)	Nakagami-m DPC/TDMA (bits/sec/Hz)	Gaussian DPC/TDMA (bits/sec/Hz)
Sabreliner with Tx2 as interferer	21.2907/ 7.5600	21.5609/ 7.6763	21.9309/ 8.0463	22.3409/ 8.4563

Sabreliner with Tx3 as interferer	21.5747/ 7.3910	21.5930/ 7.4231	21.8207/ 7.6370	22.0267/ 7.8430
Beech baron with Tx2 as interferer	21.5740/ 7.5242	21.7362/ 7.6142	22.0940/ 8.0442	22.5140/ 8.4642

c) DPC and TDMA capacity in the presence of noise

Figures 9 and 10 show the cdfs of the measured capacity in the presence of Gaussian, Cauchy and alpha stable noise. Tables 3 and 4 summarize the mean capacities obtained using the different models discussed in the previous section. the site specific 3D ray tracing software provides the best estimate to the measured capacity in both aircraft. We also observe that the mean error between simulation and measurement for the 3D ray tracing method is less than 1 % for most cases for both the DPC as well as the TDMA method. We also see that the mean error for the Nakagami-m model is less than 4% for both DPC and TDMA except. The mean error for the Gaussian channel model is less than 8 % for both DPC and TDMA.

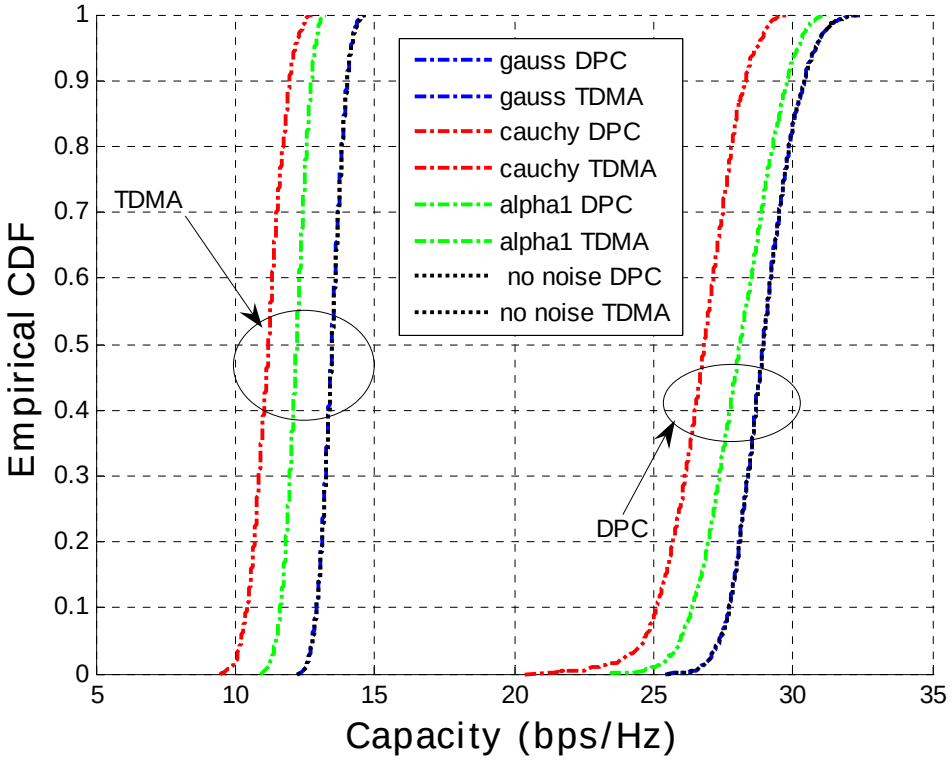

Figure 9: Empirical CDFs of the MU-MIMO capacities for the Rockwell T-39 Sabreliner with transmitter Tx1 and with three different noise scenarios. These capacities were obtained using measurements, 3D ray-tracing based Site specific modeling, and using statistical channel models like Nakagami-m and the Gaussian

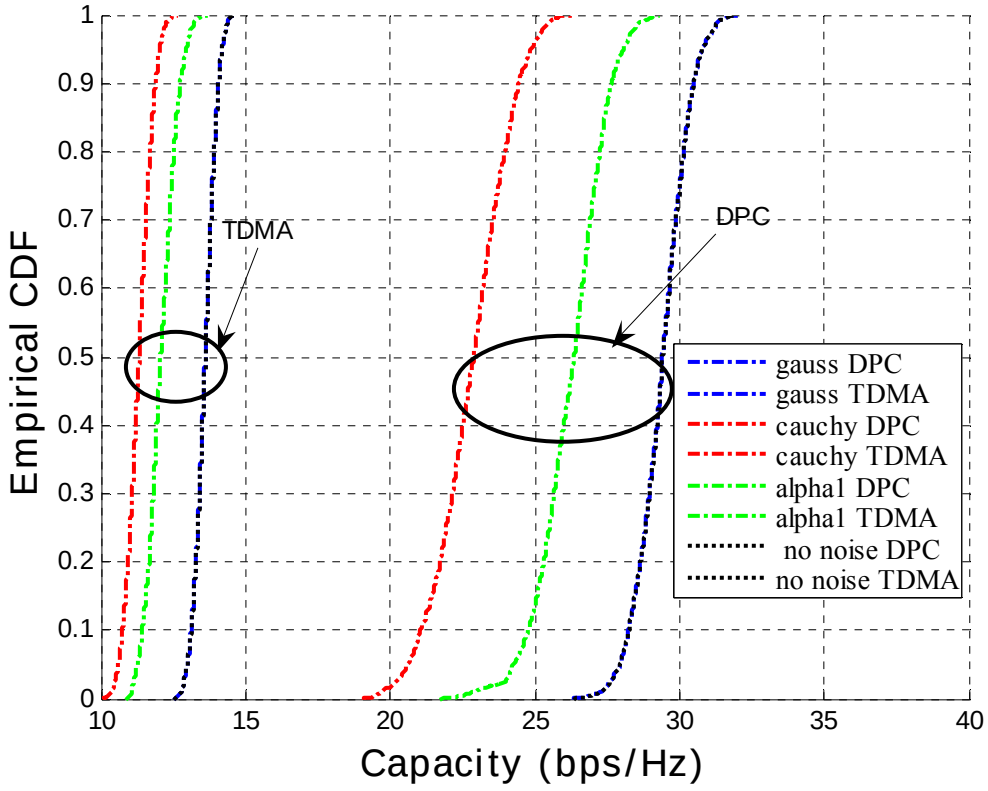

Figure 9: Empirical CDFs of the MU-MIMO capacities for the Beech baron BE 58-P with transmitter Tx1 and with three different noise scenarios. These capacities were obtained using measurements, 3D ray-tracing based Site specific modeling, and using statistical channel models like Nakagami-m and the Gaussian

Table 3: Mean Capacity results for DPC and TDMA for various noise conditions

INR= -20 dB	Measured Capacity DPC/TDMA (bits/sec/Hz)	3D ray tracing DPC/TDMA (bits/sec/Hz)	Nakagami-m DPC/TDMA (bits/sec/Hz)	Gaussian DPC/TDMA (bits/sec/Hz)
Sabreliner Gaussian	28.9910/ 13.4697	29.1165/ 13.7399	29.4865/ 14.1099	29.8365/ 14.5199
Sabreliner Cauchy	26.7393/ 11.1920	26.7408/ 11.2103	26.9853/ 11.438	27.1913/ 11.644
Sabreliner alpha stable (α=1.2)	28.1020/ 12.1919	28.1601/ 12.3541	28.5686/ 12.7119	28.9886/ 13.1319
Beech Baron Gaussian	29.4032/ 13.6038	29.4809/ 13.7201	29.8509/ 14.0901	30.2009/ 14.5001
Beech Baron Cauchy	22.8250/ 11.3244	22.8559/ 11.3565	23.071/ 11.5704	23.277/ 11.7764
Beech Baron alpha stable (α=1.2)	26.2616/ 12.0937	26.3784/ 12.1837	26.7816/ 12.6137	27.2016/ 13.0337

In the presence of noise and interference the mean capacity using the different channel models described in this paper led to similar results as in the above cases when noise and interference were considered individually. For the combined noise and interference scenario the 3D ray tracing model provided a mean capacity within 1 % of the measured capacity while the Nakagami-m and the Gaussian models estimated the capacity within 6% and 11% of the measured capacity respectively.

VII. CONCLUSION

This paper compares the measured capacity in two aircraft with a site specific 3D ray-tracing model and two statistical models for studying the effects of noise and interference in MU multi-antenna systems. Two decoding schemes viz DPC and TDMA are consideredThe site specific 3D ray-tracing model estimates the mean capacity within 1 % of the measured capacity in the presence of interference and the three types of noise sources viz: AWGN, alpha-stable and Cauchy for both aircraft. This model requires the floor plan and dimensions of the aircraft along with specific object locations (seats, walls, etc.). From the two statistical models considered in this paper we observe that the Nakagami-m model provides the best capacity estimate within 1-3% for most cases in the presence of co-channel interference and within 6% in the presence of noise and interference. The Gaussian model estimates the capacity within 3-6% for the case where we assume only interference and within 11% for the case where we assume interference and noise. The advantage of the statistical model is that it only needs information on the transmitter and receiver spacing and the Ricean K- factor when there is a strong line of sight path. This helps aircraft manufactures to predict the capacity range at various locations without performing actual measurements. From the noise plots we observe that the Cauchy noise has the worst effect of capacity and acts as the lower bound on the system capacity.

References

[1]. James R.Nagel, Sai Ananthanarayanan P.R., Alyssa Magleby Richards, Dr. Cynthia Furse," Measured multiuser MIMO capacity in aircraft", accepted for publication in IEEE Antenna and Propagation Magazine (March 2010)

UU IR Author Manuscript

[2]. J. Frolik, "A Case for Considering Hyper-Rayleigh Fading." In press, IEEE Transactions on Wireless Communications, Vol.6, No.4, April 2007

[3]. Ramya Bhagavatula, Robert W. Heath Jr., Sriram Vishwanath," Optimizing MIMO Antenna Placement and Array Configurations for Multimedia Delivery in Aircraft", IEEE 65th Vehicular Technology Conference, 2007. VTC2007-Spring, April 2007

[4]. D. Matolak and A. Chandrasekaran, "Aircraft intra-vehicular channel characterization in the 5 GHz band," in Integrated Communications, Navigation and Surveillance Conference, 2008. ICNS 2008, 2008, pp. 1–6.

[5]. G. Fraidenraich, O. Leveque, and J. Cioffi, "On the MIMO Channel Capacity for the Nakagami-m Channel," IEEE Transactions on Information Theory, vol. 54, no. 8, pp. 3752–3757, 2008.

[6]. Peruvemba R. Sai A, Alyssa Magleby, James R. Nagel, and Cynthia Furse, "MULTI-ANTENNA Wireless Communication for Aircraft Sensors," *12th Joint FAA/DOD/NASA Conference on Aging Aircraft*, Kansas City Convention Center, May 04-07, 2009

[7]. **Sai. Ananthanarayanan P.R.,** Alyssa Magleby Richards Richards, Dr. Cynthia Furse " Wireless and Surface Wave Communication for Aircraft Sensor Networks", Aircraft, Airworthiness and Sustainment conference, Austin, Tx, May 2010

[8]. R. S. Blum," MIMO Capacity with Interference", IEEE Journal on Selected Areas in Communications, Vol. 21, NO. 5,pp. 793-801, June 2003

[9]. Sai Ananthanarayanan P.R., Alyssa Magleby Richards, and Dr. Cynthia Furse," Measurement and modeling of Interference for multiple antenna system", accepted for publication in Microwave and Optical Technology Letter (April 2010)

[10]. Sai Ananthanarayanan P.R.,, Alyssa Magleby Richards, Dr. Cynthia Furse," Measurement and Modeling of Electromagnetic Interference in Aircraft Channels", submitted to IEEE Transaction on Aerospace and Electronic Systems Feb 2010

[11]. N. Jindal, W. Rhee, S. Vishwanath, S. A. Jafar,and A. Goldsmith, "Sum power iterative water-filling or multi-antenna gaussian broadcast channels," IEEE Transactions on Information Theory, vol. 51, pp. 1570–1580, April 2005.

[12]. S. Vishwanath, N. Jindal, and A. Goldsmith, "Duality, achievable rates, and sum-rate capacity of Gaussian MIMO broadcast channels," IEEE Transactions on Information Theory, vol. 49, pp. 2658–2668, October 2003.

[13]. G. Scutari, D. P. Palomar, and S. Barbarossa, "Competitive design of multiuser MIMO interference systems based on game theory: a unified framework," in Proceedings of the IEEE International Conference on Acoustics, Speech and Signal Processing (ICASSP '08), pp. 5376–5379, Las Vegas, Nev, USA, March-April 2008.

[14]. F. Kaltenberger, M. Kountouris, D. Gesbert, and R. Knopp, "Correlation and capacity of measured multi-user MIMO channels," in Proc. IEEE Intl. Symposium on Personal, Indoor and Mobile Radio Communications (PIMRC), Cannes, France, Sep. 2008.

[15]. D. Middleton, "Non-Gaussian Noise Models in Signal Processing for Telecommunications: New Methods and results for class A and class B noise models", *IEEE Transactions of Information Theory*, Vol. 45, No. 4, pp. 1129-`1147, May 1999

[16]. R.S. Blum, R.J.Kozick, and B.M.Sedler," An adaptive spatial diversity receiver for non-Gaussian interference and noise," *IEEE Trans. On Signal Processing*, vol. 47, N0. 8, pp. 2100-2111, Aug. 1999

[17]. Shahzad A Bhatti, Qingshan Shan, Ian A Glover, Robert Atkinson, Illiana E Portugues,Philip J Moore and Richard Rutherford, " Impulsive noise modelling and prediction of its impact on the performance of wlan receiver", 17th European Signal Processing Conference (EUSIPCO 2009), August 24-28, 2009

[18]. S. Y. Lim, Z. Yun, J. M. Baker, N. Celik, H.-S. Youn, and M. F. Iskander "Radio Propagation in Stairwell: Measurement and Simulation Results." IEEE Antennas and Propagation Society International Symposium. Charleston, SC, 2009.

[19]. Z. Yun, Z. Zhang, and M. F. Iskander, "A ray-tracing method based on the triangular grid approach and application to propagation prediction in urban environments," Proc IEEE Int. Symp. Information Theory (ISIT2004), vol. 50, pp. 750–758, May 2002.

[20]. D. Palchak and B. Farhang-Boroujeny, "A software defined radio testbed for MULTI-ANTENNA systems," in Proceedings of the SDR 06 Technical Conference and Product Exposition, (Orlando, FL), November 2006

[21]. Panagiotis Tsakalides, "Array Signal Processing with α-stable Distributions", PhD Thesis, University of Southern California, 1995